



Published in final edited form as:

ACS Nano. 2013 September 24; 7(9): 7711–7723. doi:10.1021/nn402241b.

Chronic Exposure to Carbon Nanotubes Induces Invasion of Human Mesothelial Cells through Matrix Metalloproteinase-2

Warangkana Lohcharoenka[§], Liying Wang[†], Todd A. Stueckle[†], Cerasela Zoica Dinu[‡], Vincent Castranova[†], Yuxin Liu[¶], and Yon Rojanasakul^{§,*}

[§]Department of Pharmaceutical Sciences and Mary Babb Randolph Cancer Center, West Virginia University, Morgantown, WV

[‡]Department of Chemical Engineering, West Virginia University, Morgantown, WV

[¶]Department of Computer Science and Electrical Engineering, West Virginia University, Morgantown, WV

[†]Pathology and Physiology Research Branch, National Institute for Occupational Safety and Health, Morgantown, WV

Abstract

Malignant mesothelioma is one of the most aggressive forms of cancer known. Recent studies have shown that carbon nanotubes (CNTs) are biopersistent and induce mesothelioma in animals, but the underlying mechanisms are not known. Here, we investigate the effect of long-term exposure to high aspect ratio CNTs on the aggressive behaviors of human pleural mesothelial cells, the primary cellular target of human lung mesothelioma. We show that chronic exposure (4 months) to single- and multi-walled CNTs induced proliferation, migration and invasion of the cells similar to that observed in asbestos-exposed cells. An upregulation of several key genes known to be important in cell invasion, notably matrix metalloproteinase-2 (MMP-2), was observed in the exposed mesothelial cells as determined by real-time PCR. Western blot and enzyme activity assays confirmed the increased expression and activity of MMP-2. Whole genome microarray analysis further indicated the importance of MMP-2 in the invasion gene signaling network of the exposed cells. Knockdown of MMP-2 in CNT and asbestos-exposed cells by shRNA-mediated gene silencing effectively inhibited the aggressive phenotypes. This study demonstrates CNT-induced cell invasion and indicates the role of MMP-2 in the process.

Keywords

Carbon nanotubes; asbestos; mesothelioma; MMP-2; mesothelial cells; cell invasion

*Corresponding Author Correspondence should be addressed to Prof. Yon Rojanasakul, West Virginia University, Department of Pharmaceutical Sciences and Mary Babb Randolph Cancer Center. Phone: 304-293-1476 yrojan@hsc.wvu.edu.

Author Contributions

The manuscript was written through contributions of all authors. All authors have given approval to the final version of the manuscript.

CONFLICT OF INTERESTS

The authors report there is no known conflict of interests.

SUPPORTING INFORMATION: Supporting Figures S1-S2 and legend. This material is available free of charge *via* the Internet at <http://pubs.acs.org>.

DISCLAIMER

The findings and conclusions in this report are those of the authors and do not necessarily represent the views of the National Institute for Occupational Safety and Health.

Carbon nanotubes (CNTs) are high aspect ratio nanoparticles (HARNs) comprising of single or concentrically stacked multi-walled graphene sheets rolled into a cylinder. CNTs have been used in a wide range of applications, in fields as diverse as electronics and medicine.^{1,2} Due to their widespread use and unknown health consequences, it is important to determine their safety especially in long-term occupational and environmental exposures. The high aspect ratio and mode of exposure of CNTs which is similar to asbestos fibers have raised a particular concern regarding the potential carcinogenicity of CNTs, especially in the pleural spaces which are key target tissues for asbestos-related diseases.³

It has been reported that after the inhalation of HARNs, they can migrate into the alveolar interstitial compartment of the lung. The low clearance rate from the interstitium would lead to biopersistence of CNTs in the lung. It has been demonstrated that 97%, 38% and 16% of CNTs remained in the lung at 1, 3 and 6 months after a single intratracheal instillation.⁴ Deposition of CNT in the alveolar airspaces, penetration through the pleural interstitium to the parietal pleura, clearance failure due to length-restricted clearance through the normal stomatal clearance system and the concomitant development of a pathogenic response in both subpleural and visceral pleura regions have previously been reported.⁵ Numerous *in vivo* studies have already demonstrated that both single-walled (SW)- and multi-walled (MW)-CNTs, when instilled into the lungs of rodents, have the potential to cause inflammation, fibrosis (scarring of the lungs) and granuloma (small nodule) formation,⁶⁻⁸ consistent with the pathogenic behaviors of asbestos. Although differences in CNT length, diameter, dispersion and functionalization impact fate, cellular uptake, persistence and pathological responses in murine lung models, similar fiber dimensions (*i.e.* high aspect ratio) and biopersistence compared to asbestos have long been recognized as important characteristics in CNT fiber pathogenicity.⁹ The translocation of a fraction of all deposited particles and fibers to the pleural space can initiate mesothelial injury and inflammation that over time leads to pleural pathology, including mesothelioma.¹⁰ The mechanism of production of pleural mesothelioma is not well understood but the contact between fibers and mesothelial cells is a reasonable supposition.

Numerous studies have demonstrated effects such as genotoxicity and inflammation following the exposure of mesothelial cells to asbestos and other fibers *in vitro*.^{11,12} Although several of the published studies investigated the acute *in vitro* effects of CNTs such as DNA breakage, alteration of cell proliferation as well as cell activation *via* AP-1, NF- κ B and AKT in both normal and malignant mesothelial cells,¹³⁻¹⁵ the effects of chronic exposure to CNTs on human mesothelial cells have not been reported. Since mesothelioma pathogenesis is a long-term multistep process, we chronically exposed human pleural mesothelial MeT5A cells to low-dose non-cytotoxic concentrations of SWCNT, MWCNT and asbestos in culture over a 4-month period. The cells were then evaluated for their proliferative, migratory and invasive properties to study the long-term cellular effects of CNTs.

Cell migration is defined as the movement of individual cells or a group of cells from one location to another. It is central to many physiological and pathological processes including wound healing, cancer, and inflammation.¹⁶ Cell invasion refers to three dimensional migration of cells as they penetrate an extracellular matrix (ECM) and is a process typically associated with cancer cell metastasis.¹⁷ Cell migration and invasion are multistep processes facilitated by a variety of factors including integrin signaling, focal-contact formation and actomyosin-dependent contractility. ECM-degrading enzymes such as matrix metalloproteinases (MMPs), urokinase plasminogen activator (uPA) and cathepsins are frequent crucial factors underlying the process of cell invasion through the surrounding tissue.¹⁸ Our study focused on comparing the effect of chronic exposure upon well-studied, high aspect ratio SWCNT and MWCNT to asbestos on the subsequent aggressive behaviors

and the underlying molecular mechanisms. Our results demonstrated for the first time aggressive transformation of human pleural mesothelial cells upon chronic exposure to CNTs and the role of MMP-2 in the process. This study strengthens the earlier finding on the mesothelioma pathogenicity of CNTs and supports the prudent adoption of prevention strategies and implementation of exposure control.

RESULTS

Chronic CNT exposure induces cell proliferation and aggressive behaviors of mesothelial cells

Non-tumorigenic human lung mesothelial MeT5A cells were continuously exposed to sub-cytotoxic concentration ($0.02 \mu\text{g}/\text{cm}^2$) of SWCNT, MWCNT, crocidolite asbestos, or vehicle control for up to 4 months as described under *Materials and Methods*. This relatively low concentration was relevant to lung burdens achieved after *in vivo* exposure of mice to CNTs.¹⁹⁻²¹ The exposed cells were evaluated for their growth characteristics by Cyquant® cell proliferation and Hoechst 33342 assays, and for their aggressive behaviors by Transwell® cell migration and invasion assays. Analysis of cell growth characteristics by Cyquant® assay shows that mesothelial cells treated with SWCNT, MWCNT, or asbestos exhibited a significantly higher growth rate than Survanta (vehicle)- or saline-treated controls (**Figure 1A**). Microscopic analysis of the cells by Hoechst assay confirmed the above finding (**Figure 1B**) and indicated that long-term exposure of mesothelial cells to SWCNT, MWCNT, or asbestos induced cell growth. The increase in cell growth was not observed until after 16 weeks of exposure.

The aggressive behaviors of particle-exposed cells were assessed by cell invasion and migration assays. Both SWCNT and MWCNT-exposed cells demonstrated a significant increase in cell invasion (5.4 to 6.3-fold) and migration (2.5 to 2.7-fold) as compared to Survanta-treated control (**Figure 1, C and D**). Likewise, asbestos-exposed cells exhibited an increase in cell motility as compared to saline-treated control, but to a lesser extent than the SWCNT and MWCNT-exposed cells. These results indicate that high-aspect ratio SWCNT and MWCNT, like asbestos, can induce accelerated cell growth and invasiveness, which are key cancer phenotypes that may contribute to their mesothelioma pathogenicity.

Increased MMP-2 expression and activity in CNT-transformed mesothelial cells

To understand the underlying mechanism of CNT-induced cell invasiveness, we investigated 12 selected genes known to be involved in the regulation of cell migration and invasion, including *CAV1*, *COL4A2*, *MMP-9*, *MMP-2*, *RAC1*, *STAT3*, *MET*, *NME1*, *SERPINE1*, *TIMP1*, *AKT1* and *MAPK3* by quantitative real-time PCR (qPCR). Among these, *MMP-2* (also known as gelatinase A) was found to be most strikingly up-regulated in both SWCNT and MWCNT-transformed cells as compared to control cells. In SWCNT cells, a 51-fold increase in *MMP-2* mRNA expression level was observed, whereas a 23-fold increase was seen in MWCNT cells (**Figure 2A**). Other genes that were slightly or moderately upregulated in these cells include *CAV1*, *SERPINE1*, *TIMP1*, *AKT1*, and *MAPK3*. In asbestos-transformed cells, *MMP-2* and *SERPINE1* were most strongly up-regulated, followed by *CAV1* and *AKT1* (**Figure 2B**).

Based on its high expression profile in both CNT- and asbestos-transformed cells, we further investigated MMP-2. MMP-2 protein expression and gelatinolytic activity in SWCNT, MWCNT, and asbestos cells were examined by Western blotting, gelatin zymography, and immunofluorescence. Consistent with the mRNA expression data, MMP-2 protein expression and gelatinolytic activity were up-regulated in SWCNT, MWCNT and asbestos-transformed cells (**Figure 3, A and B**). Immunofluorescence staining of MMP-2 in these

cells showed increased fluorescence intensity in SWCNT, MWCNT, and asbestos cells (136.1, 112.4 and 97.1 units/square inches, respectively) over control levels (94.5 and 61.8 units/square inches) in Survanta and saline-treated control cells (**Figure 3C**).

Gene signaling network analysis reveals the importance of MMP-2 in CNT-induced invasion of mesothelial cells

To gain an insight into gene signaling contributing to the invasive phenotype of CNT and asbestos-transformed cells, whole genome microarray analysis of the cells were conducted and analyzed for gene signaling networks (GSNs) by Ingenuity Pathway Analysis (IPA). GSNs for cell invasion of SWCNT and MWCNT cells were very similar and are shown in **Figure 4A**. Interestingly, *MMP-2* occupied a focal position of the GSNs in both CNT- and asbestos-transformed cells. Other signaling hub genes with a first order connection to *MMP-2* in the invasion GSNs include *PLAU*, *STAT3*, *AKT1* and *VEGFA*. Invasion GSN of asbestos-transformed cells was distinct and indicated *CAVI* and *CCL2* up-regulation and *EGFR* and *TIMP2* down-regulation (**Figure 4B**). *CAVI* and *CCL2* were however common hub genes found in the invasion GSNs of both CNT and asbestos cells. These results provide molecular evidence supporting the invasive properties of CNT and asbestos-transformed cells through some common and distinct gene signaling pathways.

Knockdown of MMP-2 reduces the invasiveness of CNT-transformed mesothelial cells

To demonstrate the functional role of MMP-2 in the invasiveness of CNT-transformed cells, gene knockdown experiments were conducted in SWCNT, MWCNT and asbestos-transformed cells. The cells were stably transfected with MMP-2 short-hairpin (sh)RNA plasmid and analyzed for MMP-2 gene and protein expression as well as gelatinase activity by qPCR, Western blotting, gelatin zymography, and immunofluorescence. Real-time PCR analysis of mRNA expression showed a substantial (73-82%) reduction in *MMP-2* mRNA in the shRNA-transfected SWCNT, MWCNT, and asbestos-transformed cells as compared to their respective controls (**Figure 5A**). Western blot and gelatin zymography studies similarly indicated a reduction in MMP-2 protein expression and enzyme activity in the shRNA-transfected cells (**Figure 5, B and C**). Immunofluorescence studies further showed a corresponding reduction in MMP-2 immunofluorescence intensity in the three shRNA-transfected cells vs. controls (**Figure 5D**). Together, these results indicate effective knockdown of MMP-2 expression and enzyme activity in the SWCNT, MWCNT, and asbestos-transformed mesothelial cells.

To determine whether MMP-2 plays a role in the aggressive behavior of CNT and asbestos-transformed cells, cell invasion and migration assays of the MMP-2 knockdown and vector-transfected control cells were performed. A substantial (60-90%) decrease in cell invasion was observed with the MMP-2 knockdown cells as compared to control cells (**Figure 6A**). Likewise, knocking down of MMP-2 in the CNT and asbestos-transformed cells has an inhibitory effect on the migratory activity of the cells (**Figure 6B**).

DISCUSSION

Pleural mesothelioma is one of the most aggressive forms of cancer that develops from transformed mesothelial cells originating in the pleura, the protective lining of the lungs and internal chest wall. The objective of this study was to investigate the effect of long-term exposure to sub-cytotoxic dose of CNTs on the aggressive behavior of human mesothelial cells, the pleural lining cells which has been reported to be strongly reactive in response to fiber exposure.²² Here, we compared a set of well-studied SWCNT and MWCNT high-aspect ratio particles to asbestos, a positive control HARN particle, for their abilities to cause aggressive behavior in human mesothelial cells. CNTs and other HARNs have been

reported to be translocated to the pleural space and their inadequate clearance from this site is considered a key determinant of their pathogenicity.²³ We demonstrated here for the first time that chronic exposure of human pleural mesothelial cells to CNTs induce proliferative and aggressive phenotypes of the cells, as indicated by their increased growth rate, migration, and invasion (**Figure 1**). Proliferative and genetic changes after cellular entry of SWCNT and MWCNT both *in vitro* and *in vivo* have been reported through a variety of mechanisms. One of these mechanisms is the interaction between the nanotubes and structural elements of the cell with apparent binding to the cytoskeleton, telomeric DNA, and G-C rich DNA sequences in the chromosomes.^{24,25} A study of lung epithelial cells exposed to CNTs demonstrated multipolar mitotic spindles, fragmented centrosomes and aneuploid chromosomes. The increased multipolar mitotic spindles were associated with an increased number of cells in the G2 phase of mitosis leading to increased proliferation of CNT-exposed cells. These genetic alterations may be transmitted to daughter cells and have been suggested to be important in both tumorigenesis and tumor progression.²⁶ In the case of asbestos, it was reported to cause cell injury and induce a transient proliferative response in mesothelial cells after a single exposure. Moreover, repeated exposures may induce prolonged injury, cytokine production and mesothelial proliferation without necessarily involving direct action of asbestos fibers on these cells at the pleura.²⁷ Oxidative stress induction has also been implicated to trigger cell proliferation and injury upon asbestos exposure. The high iron content of asbestos fibers appeared to be critical to the genesis of reactive oxygen species (ROS), including the highly DNA-damaging hydroxyl radical. These reactive species can initiate aberrant transcriptional responses leading to the increase in cell proliferation and transformation.²⁸ An increase in ROS production along with the depletion and loss of protective mechanism against ROS in lung cells upon CNT exposure has been demonstrated as well. This incidence has been linked to CNT-induced inflammation, genotoxicity, fibrosis and granulomas formation in mice.²⁹ Consistently, our 4-month CNT- and asbestos-exposed cells exhibit increased ROS production and reduced superoxide dismutase-1 (SOD-1) expression (**Supporting figure S1**).

Increased cell invasion and migration were observed in mesothelial cells chronically exposed to CNTs and asbestos (**Figure 1B**). Cell migration and invasion are crucial steps in many physiological events such as embryogenesis, morphogenesis, angiogenesis, wound healing, and inflammation. However, cell migration and invasion are also implicated in many pathological processes such as carcinogenesis and metastasis, and have been used to assess the aggressive and malignant phenotypes of the cells.^{30,31} We previously reported the malignant transformation and tumorigenesis of human lung epithelial cells after long-term exposure to SWCNT as well as the induction of cancer phenotypes including cell invasion and migration, but the genes involved in the increased migration and invasion are not known.³² Meanwhile, asbestos-induced mesothelioma, a highly invasive type of cancer, has been reported to express high levels of growth factor receptor and oncogenes especially *c-FOS* and *c-JUN*.³³ Ultrafine carbon black (UFCB) was used as a comparative non-HARN particle in this study. With the same dispersion method as CNT, long-term UFCB exposure induced mesothelial cell growth equivalent to CNT and asbestos (**Supporting figure S2A**). This is in conformity with the previously reported stimulatory effect of UFCB on human airway epithelial cell proliferation *via* the process of soluble heparin-binding (HB)-EGF release and concomitant activation of epidermal growth factor receptor (EGFR) and ERK cascade.³⁴ Although UFCB could stimulate cell proliferation, the effect on cell invasion and migration was significantly lower than SWCNT and MWCNT (**Supporting figure S2B and S2C**). Thus, UFCB-exposed cells were excluded from further study.

Since migration and invasion of cells through tissues is a highly coordinated process that involves several interdependent steps and various specific genes,³⁵ we tested 12 selected genes most frequently associated with cell migration and invasion using RT-qPCR (**Figure**

2). Both SWCNT and MWCNT-exposed cells exhibited a dramatic increase in *MMP-2* expression, which is the highest among the genes tested. Increased *MMP-2* protein expression and gelatinolytic activity were also observed with the CNT-exposed cells, as determined by Western blotting, immunofluorescence, and gelatin zymography (**Figure 3**). Several MMP genes have been reported to be up-regulated in mice after pulmonary CNT exposure and have been shown to be associated in early lung fibrotic and subchronic tissue damage induction.^{36,37} *MMPs* are signature invasion marker genes that encode proteins involved in the degradation of ECM and are typically highly active during lung cancer development and progression.³⁸ *MMP-2* is also highly up-regulated in cells chronically exposed to asbestos (**Figure 3**). This finding is consistent with a previous report showing an increase in *MMP-2*, *MMP-7*, *MMP-9*, *MMP-12* and *MMP-13* expression in the lungs of mice after intra-tracheal instillation of asbestos and suggests the contribution of MMPs on asbestos-induced lung inflammation and fibrosis, particularly *MMP-2*, which is increased in the fibrotic phase and also in the fibrotic region.³⁹

It is known that degradation and remodeling of ECM are essential to cell migration, invasion and metastasis. These processes are mediated by several proteolytic enzymes, most notably MMPs.⁴⁰ MMPs belong to a family of zinc-dependent endopeptidases, highly conserved and structurally related enzymes capable of degrading many components of basement membrane and ECM.⁴¹ They can be divided into different classes according to their sequence homology, substrate specificity, and cellular localization. The 72 kDa *MMP-2* (gelatinase A) has an important role in basement membrane turnover due to its specific activity to collagen type IV or gelatin which is the major structural protein of the basement membrane. Its degradation plays a role in cell invasion of the vasculature and is considered to have a key role in metastasis. *MMP-2* expression has been associated with the invasiveness of many cancer cell lines and is elevated in high-grade tumors, specifically at the invasive front and in vascular invasion.^{42,43} Inhibition of *MMP-2* activity by *MMP-2* inhibitors has been reported to suppress local invasiveness of various carcinomas.⁴⁴⁻⁴⁶ Furthermore, elevated *MMP-2* levels has been used for prognosis of invasive and metastatic lung cancers and the reduction of cancer cell colonization in the lung of *MMP-2* deficient mice than wild-type mice has been reported.⁴⁷

Whole genome microarray and IPA were used to hypothesize pro-invasion gene networks of chronic CNT- and asbestos-exposed mesothelial cells (**Figure 4**). The importance of *MMP-2* encoded genes in both networks is indicated by focal position of *MMP-2* in both CNT- and asbestos-induced networks with a slight difference in some associated hub genes. In CNT-induced pro-invasion network, other signaling hub genes with first order linkage to *MMP-2* include *PLAU*, *STAT3*, *AKT1* and *VEGFA*. Urokinase-plasminogen activator or *PLAU* gene is known to encode uPA, the protease which degrades ECM and plays critical roles in cell migration, tissue remodeling, angiogenesis, tumor invasion and metastasis.^{48,49} Plasminogen activators convert plasminogen to plasmin, which works more efficiently in proteolysis of the fibrin, whereas the MMPs family is the main proteases for fibronectin, laminin, elastin, and collagens. In addition, plasminogen activators activate several MMPs and could also facilitate the MMPs activities. The overlapping contribution of uPA and *MMP-2* in cell migration and invasion has been reported to be correlated with more aggressive metastatic behavior of cancer cells.⁵⁰ *STAT3* has been shown to regulate tumor growth, angiogenesis and metastasis of several cancer types including non-small cell lung cancer and mesothelioma. *STAT3* activation is also contributed to oncogenesis. The role of activated *STAT3* in oncogenesis is manifested presumably through its role in the expression of many key genes that regulate multiple aspects of tumor cell survival, growth, angiogenesis and evasion of immune surveillance such as cyclin D1, c-myc, vascular endothelial growth factor (VEGF), and *IP-10*.⁵¹ Several studies have shown that *MMP-2* transcription is directly regulated by *STAT3*. It has been reported that *STAT3* can bind to the

promoter of *MMP-2* gene and up-regulates its expression. Blockade of activated *STAT3* by ectopic expression of dominant negative *STAT3* suppresses *MMP-2* expression and invasiveness of tumor cells, inhibits tumor growth, and prevents metastasis in nude mice.^{52,53} Phosphatidylinositol-3-kinase (*PI3K*)-*AKT* signaling plays a prominent role in several processes considered the hallmark of cancer. It has been reported that *AKT* promotes cancer cell invasion *via* increased motility and MMP production. MMP-driven metastasis has also been reported to correlate with phosphorylation of ERK1/2 and PI3K/AKT. *AKT1* is one of three mammalian isoforms and is activated by several growth factor pathways and implicate in a variety of cellular functions, such as survival, transcription, and translation. The correlation between invasion activity of *AKT1* expressing cells and the increase of *MMP-2* expression and activation has been reported. It was suggested that the invasive behavior induced by *AKT1* may result from inhibition of *MMP-2* degradation by the proteasome pathway.^{54,55} *VEGF* is a well known regulator of tumor progression, angiogenesis and metastasis. Positive correlation between *VEGF* and *MMP-2* expression has been reported in lung carcinoma cells. *MMP-2* has been found to regulate the production of *VEGF* and *VEGF* overexpression may promote the expression of *MMP-2* as well.⁵⁶ For asbestos-induced pro-invasion network, the important upstream genes that may regulate *MMP-2* production are *CAVI*, *TIMP2* and *CCL2*. Down-regulation of tissue inhibitor of *MMP-2* (*TIMP-2*) is shown in the network. An imbalance between the proteolytic activity of *MMP-2* and *TIMP-2* is responsible for the degradation of ECM components, a key step in tumor invasion and metastasis. Several studies have reported that the invasion and metastasis dissemination is facilitated by increased levels of *MMP-2* and/or decreased levels of *TIMP-2*, either of which can shift the balance of proteolysis or cause basement membrane degradation. This is the key point for the beginning of tumor spread and metastasis formation, which have a positive correlation with *MMP-2* proteolytic activity.⁵⁷⁻⁵⁹ *CAVI* and *CCL2* are over-expressed in both CNT and asbestos-induced pro-invasion GSN. Caveolin-1 (*CAV1*) is a major component of cell surface invaginations caveolae which could interact with many signal molecules such as EGFR, IR, PDGF receptor and play an important role in cell adhesion and growth factor mediated signal transduction. Recently, *CAVI* has been identified as a metastasis-associated gene and *CAVI* up-regulation is associated with highly migratory and invasive cancer cells *via* the induction of *MMP-9* production and *MMP-2* activation.⁶⁰ Monocyte chemoattractant protein-1 (*MCP-1*) encoded by *CCL2* gene is an inflammatory biomarker known to be overproduced after asbestos and CNT exposure. Induction of *MCP-1* mRNA expression in rat pleural mesothelial cells after crocidolite and chrysotile asbestos exposure and the increase of *MCP-1* protein in the pleural lavage fluid of exposed rats have been reported.⁶¹ Significant elevations of several cytokines and chemokines including *MCP-1* in bronchoalveolar lavage fluid were also noted after pharyngeal instillation.⁶² Cell migration and invasion driven by *MCP-1* has been described and several studies revealed that *MCP-1* could enhance *MMP-2* activity.⁶³ Further examination of microarray data showed the increase of oxidative phosphorylation reactions associated with mitochondrial metabolism function which correlated with the increase of ROS production and reduction of *SOD-1* expression in both CNT- and asbestos-exposed cells. Since ROS was known to activate several upstream pathways that mediate *MMP-2* activity *via* different signal molecules and genes including *AKT1* and *MCP-1* which were found to be up-regulated in CNT- and asbestos-induced pro-invasion GSN,^{64,65} oxidative stress induction may be a factor involved in CNT- and asbestos-induced *MMP-2* activation.

To confirm the importance of *MMP-2* in cell migration and invasion caused by chronic exposure to CNTs and asbestos, SWCNT, MWCNT and asbestos-transformed cells were transfected with *MMP-2* shRNA or control plasmid, and *MMP-2* mRNA and protein expression as well as enzyme activity were determined by qPCR, Western blotting, immunofluorescence, and gelatin zymography (**Figure 5**). As compared to control transfectants, all *MMP-2* shRNA transfectants exhibited substantially reduced *MMP-2*

expression and activity. Functionally, the MMP-2 knockdown cells showed greatly reduced invasive and migratory properties as compared to their vector-transfected controls (**Figure 6**). Collectively, the observation that MMP-2 is upregulated in all CNT- and asbestos-exposed cells and the finding that downregulation of MMP-2 in these cells consistently inhibits their aggressive behaviors suggest a common and important role of MMP-2 in HARN-induced mesothelial toxicities. Concerns over rapid development of new nanomaterial technologies and the risks to human health, this long-term *in vitro* exposure model can provide rapid, robust and high throughput assessments for future research on mesothelioma hazard of nanomaterials.

CONCLUSION

In summary, we demonstrated that chronic exposure of human pleural mesothelial cells to CNTs or asbestos induced cell transformation with cancer-like properties such as rapid growth and increased cell invasion and migration. The described *in vitro* exposure model could potentially be used to predict mesothelioma pathogenicity of nanomaterials and to aid mechanistic studies of the cellular and molecular events leading to mesothelioma. Using the described model, we identified several genes involved in the transformation and aggressive behaviors of chronic CNT and asbestos-exposed mesothelial cells. Among these, MMP-2 was identified as a key regulator of the aggressive behaviors of the transformed cells based on gene expression and knockdown data. Gene signaling networks obtained from microarray data and IPA confirmed the importance of MMP-2 in cell invasion induced by chronic CNT and asbestos exposure. Other genes involved in the CNT-induced invasion network include *PLAU*, *STAT3*, *AKT1* and *VEGFA*, whereas *CAVI*, *EGFR*, *TIMP2* and *CCL2* are altered in the asbestos-induced invasion network. These genes have the potential to regulate MMP-2 production and activity in CNT and asbestos-transformed cells.

MATERIALS AND METHODS

Cell Culture and Chronic Exposure

Human pleural mesothelial MeT5A cells were acquired from American Type Culture Collection (Manassas, VA) and maintained in M199 medium (Life Technologies, Grand Island, NY) with 5% fetal bovine serum (FBS), 2 mM L-glutamine, 100 U/mL penicillin/streptomycin, 1 μ g/mL EGF and 50 μ g/mL hydrocortisone. Cell cultures were performed in a humidified atmosphere of 5% CO₂ at 37°C. SWCNT, synthesized using high-pressure carbon monoxide disproportionate process (HiPCO), were obtained from Carbon Nanotechnology (CNI, Houston, TX). MWCNT were provided by Mitsui & Company (MWNT-7, lot #05072001K28) and crocidolite asbestos (CAS# 12001-28-4) was obtained from the Kalahari Desert in South Africa by the National Institute of Environmental Health Sciences (Research Triangle Park, NC). UFCB was acquired from Cabot (Edison, NJ). All tested particles were characterized as previously described in our recent study.⁶⁶ Elemental analysis of the supplied SWCNT by nitric acid dissolution and inductively coupled plasma-atomic emission spectrometry (ICP-AES, NMAM #7300) showed that SWCNT were 99% elemental carbon and contained less than 1% w/w of contaminants while MWCNT contained 0.41% w/w metal impurity. Both SWCNT and MWCNT possessed 0.32% Fe and 0.41% Na ion impurities. Diameter and length distribution of dispersed particles were measured by field emission scanning electron microscopy (FESEM, model S-4800; Hitachi, Tokyo, Japan). Mean length of SWCNT, MWCNT and asbestos was 1.42, 4.90 and 10 μ m while mean width was 0.38, 0.08 and 0.21 μ m, respectively. UFCB possessed <1% w/w metal impurities with a dry and medium dispersed width of 37 and 700 nm, respectively. All particles possessed surface areas between 9.8-43 m²/g except SWCNT which was 10 to 100 folds greater (400-1040 m²/g).

The cells were continuously exposed to a sub-cytotoxic concentration ($0.02 \mu\text{g}/\text{cm}^2$) of SWCNT, MWCNT, crocidolite asbestos, UFCB or vehicle for 4 months following the method previously described.⁶⁷ Briefly, $0.1 \text{ mg}/\text{mL}$ stocks of SWCNT and MWCNT in phosphate buffer saline (PBS) containing $150 \mu\text{g}/\text{mL}$ Survanta® (Abbott Laboratories, Abbott Park, IL) were sonicated and diluted in media ($0.1 \mu\text{g}/\text{mL}$) prior to cell exposure. This method of dispersion mimics natural lung surfactant content, is non-toxic and effective in dispersing CNTs to the size of aerosolized particles reported in the workplace.⁶⁸ Crocidolite asbestos was sonicated in culture medium without the dispersant. MeT5A cells (1×10^4) were exposed to the dispersed particles every 3 days following a PBS wash and passaged once per week to initial seeding densities. Vehicle-only exposed cells and passage-matched control cells were used as controls. Calculation of the exposure dose was based on *in vivo* SWCNT and MWCNT aspiration and inhalation total lung burden dose of $20 \mu\text{g}/\text{mouse}$ previously reported.⁶⁹ The penetration of CNT from lung periphery through the visceral pleura into the pleural space after aspiration exposure has been quantified and 0.6% of the deposited fiber burden was found to reach the visceral pleura. From the estimated pleural surface area of 5 cm^2 in mice, the possible dose of CNT per cm^2 of visceral pleura is approximately $0.024 \mu\text{g}/\text{cm}^2$.

Cell Proliferation Assays

Cell proliferation was quantified over a 72 h period using Cyquant® cell proliferation assay kit (Invitrogen, Grand Island, NY) and Hoechst 33342 vital staining. In the Cyquant® assay, cells were seeded ($5,000 \text{ cells}/\text{well}$) in quadruplicate in a 96-well plate in a normal growth medium. Cells were incubated for various times before the replacement of media with $100 \mu\text{L}$ of 1X Cyquant® dye solution and incubated for 1 h. Each sample's fluorescence intensity was measured using a fluorescence microplate reader at a 485 nm excitation and 520 nm emission (FLUOstar OPTIMA, BMG Labtech, Durham, NC). In the Hoechst assay, $10 \text{ mg}/\text{mL}$ stock solution of Hoechst 33342 was diluted to $5 \mu\text{g}/\text{mL}$ in PBS and $100 \mu\text{L}$ of the $5 \mu\text{g}/\text{mL}$ solution was added into each well. The cells were incubated for 30 min before visualization under a fluorescence microscope (Leica Microsystems, Bannockburn, IL).

Migration and Invasion Assays

Cell migration and invasion were determined in the 24-well plate Transwell® system with $8\text{-}\mu\text{m}$ pore size polycarbonate filter and BD Matrigel® invasion chamber (BD Biosciences, NJ). Briefly, cells at the density of 1.5×10^4 cells per well (migration) or 3×10^4 cells per well (invasion) were seeded into the upper chamber of the Transwell® unit in serum-free medium. The lower chamber of the unit was added with a normal growth medium containing 5% FBS. The unit was incubated at 37°C in a 5% CO_2 atmosphere for 48 h. The non-migrating or non-invading cells were removed from the inside of insert with a cotton swab. Cells that migrated or invaded to the lower side of the membrane were fixed and stained with Diff-Quik® (Dade Behring, Newark, DE). Inserts were visualized and scored under a light microscope (Leica DM, IL).

Quantitative Real-Time PCR of Motility Genes

The expression of 12 selected genes known to be involved in the regulation of cell migration and invasion including CAV1, COL4A2, MMP-9, MMP-2, RAC1, STAT3, MET, NME1, SERPINE1, TIMP1, AKT1 and MAPK3 was analyzed. Total RNA was isolated from cells using RNeasy mini kit (Qiagen, Valencia, CA), according to the manufacturer's instructions. The extracted RNA was then reverse transcribed into cDNA by high capacity RNA to cDNA kit (Applied Biosystems, Carlsbad, CA). After the reverse transcription reaction was finished, $10 \mu\text{L}$ of diluted cDNA product (final cDNA quantity 100 ng) was mixed with $10 \mu\text{L}$ of Taqman® master mix (Applied Biosystems) and transferred into Taqman® array plate

(Applied Biosystems). Quantification of the PCR products was performed by NFQ-FAM® method using the Applied Biosystems 7500 Real-Time PCR system with the following profile: 1 cycle at 94°C for 2 min, 40 cycles at 94°C for 15 sec, 60°C for 1 min, 72°C for 1 min. Data analysis was performed using the ABI sequence detection software (Applied Biosystems) by relative quantification. The threshold cycle (Ct), which is defined as the cycle at which PCR amplification reaches a significant value, is given as the mean value. The relative expression of each mRNA was calculated by the ΔCt method, where ΔCt is the value obtained by subtracting the Ct value of the housekeeping gene *18S* mRNA from the Ct value of the target mRNA. The amount of the target relative to *18S* mRNA was expressed as $2^{-\Delta\text{Ct}}$.

Western Blot Analysis

Cells were washed twice with ice-cold PBS and incubated in lysis buffer containing 20 mM Tris-HCl (pH 7.5), 1% Triton X-100, 150 mM NaCl, 10% glycerol, 1 mM Na_3VO_4 , 50 mM NaF, 100 mM phenylmethylsulfonyl fluoride, and a commercial protease inhibitor mixture (Roche Molecular Biochemicals, Indianapolis, IN) at 4°C for 20 min. Cell lysates were collected and analyzed for protein content using the BCA protein assay kit (Pierce Biotechnology, Rockford, IL). Samples containing 50 μg of cell lysate proteins per lane were resolved under denaturing conditions by 10% sodium dodecyl sulfate-polyacrylamide gel electrophoresis (SDS-PAGE) along with EZ-run pre-stained protein ladder (Fisher Scientific, Pittsburgh, PA) and transferred onto PVDF membranes (Invitrogen, Carlsbad, CA). The transferred membranes were blocked for 1 h in 5% nonfat dry milk in TBST (25 mM Tris-HCl, pH 7.4, 125 mM NaCl, 0.05% Tween 20) and incubated with the appropriate primary antibodies at 4°C overnight. Membranes were washed twice with TBST for 10 min and incubated with horseradish peroxidase-coupled isotype-specific secondary antibodies for 1.5 h at room temperature. The immune complexes were detected by enhanced chemiluminescence detection system (Amersham Biosciences, Piscataway, NJ) and quantified using analyst/PC densitometry software (Bio-Rad Laboratories, Hercules, CA).

Gelatinolytic Activity

Cells at the density of 1×10^5 cells/well were seeded into a 6-well plate with 1 mL completed M199 medium and cultured for 24 h. Cell supernatants were collected and determined for total secreted protein concentrations and analyzed by zymography. Secreted proteins at 5 μg per lane were separated by electrophoresis in SDS-polyacrylamide gels containing 0.1% gelatin. After electrophoresis, gels were renatured by incubation in 2.5% Triton X-100 for 30 min, incubated overnight in substrate buffer (50 mM Tris-HCl, pH 7.5, containing 10 mM CaCl_2) at 37°C, and stained with 0.5% Coomassie brilliant blue. Recombinant MMP-2 (Raybiotech, Norcross, GA) was used as a positive control. A clear zone in the blue background indicated the presence of gelatinolytic activity. Computerized densitometry was used to evaluate enzymatic activity.

Immunofluorescence Staining

Cellular MMP-2 expression was visualized by immunofluorescence microscopy (Zeiss LSM 510 Axiovert 100M, Zeiss, Thornwood, NY) as previously described.⁷⁰ Briefly, cells were cultured to confluence on glass cover slips and fixed in 4% paraformaldehyde in PBS. The samples were rinsed three times, permeabilized with 1.2% Triton X-100 for 5 min, rinsed three times and blocked with 1% bovine serum albumin (BSA) in PBS for 1 h before staining with 1:200 MMP-2 primary antibody (Abcam, Cambridge, MA) followed by Alexa Fluor-conjugated secondary antibody (Invitrogen, Carlsbad, CA). The stained cells were mounted with ProLong® gold antifade reagent with DAPI (Invitrogen, Carlsbad, CA) and visualized by fluorescence microscopy. All microscopic exposure conditions were set the

same between samples for fluorescence intensity comparison using Image J Java-based image processing program. Fluorescence intensity per square inches was calculated.

Whole Genome Expression Microarray and Ingenuity Pathway Analysis

Whole genome expression for each treatment was determined using high-throughput mRNA microarray analysis following MIAME guidelines as described previously.⁷¹ Briefly, cells from each treatment (1×10^6 in 6-cm plate) were lysed in triplicate using TRIzol® reagent (Life Technologies, Grand Island, NY). Total RNA was isolated, purified and quantified using Nanodrop ND-1000 (Thermo Scientific, Rockford, IL). RNA was tested for purity and DNA contamination using A260/A280 ratio and standard denaturing agarose gel electrophoresis. Double-stranded cDNA was synthesized using Invitrogen Superscript ds-cDNA synthesis kit, cleaned, and Cy3 labeled by a NimbleGen One-Color DNA labeling kit following the manufacturer's protocol (Roche NimbleGen, Madison, WI). Samples were hybridized to NimbleGen Human 12×135 k Gene Expression Array using the NimbleGen Hybridization System. The slides were then washed with NimbleGen wash buffer, dried and scanned with Axon GenePix 4000B microarray scanner (Molecular Devices Corporation, Sunnyvale, CA). Finally, raw data intensities were extracted from the aligned scanned images and normalized through quantile normalization and Robust Multichip Average method in NimbleGen v2.5. Gene level files were imported into Agilent GeneSpring GX (v12.1) for analysis. Genes with <50.0 intensity were removed from further analysis. Volcano plots were constructed using two sample *t*-tests assuming equal variance ($p < 0.05$) with a fold-change screening (± 2 -fold) to identify differentially expressed genes (DEGs) for SWCNT and MWCNT compared to dispersant-treated cells, and asbestos compared to control cells. Microarray expression data was compared to qPCR invasion gene data to validate the microarray. All gene expression data were deposited to NCBI's Gene Expression Omnibus and is accessible *via* accession number (GenBank ID: GSE48855).

To investigate the impact of chronic CNT or asbestos exposure on gene signaling promoting invasive behavior, DEGs were analyzed using Ingenuity Pathway Analysis (IPA, version Fall 2012; Redwood City, CA). Tab-delimited text files containing gene IDs, expression data and *t*-test *p*-values were uploaded into IPA. Gene signaling networks (GSNs) associated with promoting invasion were created and mapped. Genes were included in the GSN if they promoted invasion and were overexpressed or if they inhibited invasion and were underexpressed.

MMP-2 Short-Hairpin RNA Transfection

Cells were transfected with pre-designed MMP-2 shRNA or scrambled vector (SureSilencing®, SABiosciences, Frederick, MD) according to the manufacturer's protocol. Stable MMP-2 knockdown clones were generated by puromycin selection ($0.2 \mu\text{g/mL}$, Life Technologies, Grand Island, NY). Expression of MMP-2 in the shRNA and scrambled vector-transfected cells was determined by qPCR and Western blotting as described above.

Statistical Analysis

Results are expressed as means \pm SD. All values were derived from at least three independent experiments. Differences between groups were assessed by one-way analysis of variance (ANOVA). If the variances between groups were homogenous, groups were subjected to the multiple comparison Dunnett's test. If the variances were not homogeneous, groups were compared by the Mann-Whitney test. Differences were considered significant if *P* values were <0.05 .

Supplementary Material

Refer to Web version on PubMed Central for supplementary material.

Acknowledgments

This work was supported by grants from the National Science Foundation (EPS-1003907) and National Institutes of Health (R01-HL095579). Imaging experiments were performed in the West Virginia University Imaging Facility, which is supported in part by the Mary Babb Randolph Cancer Center and NIH grants P20 RR016440, P30 RR032138/GM103488 and P20 RR016477.

ABBREVIATIONS

CNT	carbon nanotube
SWCNT	single-walled CNT
MWCNT	multi-walled CNT
DEG	differentially expressed gene
HARN	high aspect ratio nanoparticle
ECM	extracellular matrix
GSN	gene signaling network
MMP	matrix metalloproteinase
uPA	urokinase plasminogen activator
DEG	differentially expressed gene
IPA	Ingenuity Pathway Analysis
PCR	polymerase chain reaction

REFERENCES

1. Shvedova AA, Kisin ER, Porter D, Schulte P, Kagan VE, Fadeel B, Castranova V. Mechanisms of Pulmonary Toxicity and Medical Applications of Carbon Nanotubes: Two Faces of Janus? *Pharmacol. Ther.* 2009; 121:192–204. [PubMed: 19103221]
2. Helland A, Wick P, Koehler A, Schmid K, Som C. Reviewing the Environmental and Human Health Knowledge Base of Carbon Nanotubes. *Environ. Health Perspect.* 2007; 115:1125–1131.
3. Donaldson K, Murphy F, Schinwald A, Duffin R, Poland CA. Identifying the Pulmonary Hazard of High Aspect Ratio Nanoparticles to Enable their Safety-by-Design. *Nanomedicine.* 2011; 6:143–156. [PubMed: 21182425]
4. Elgrabli D, Floriani M, Abella-Gallart S, Meunier L, Gamez C, Delalain P, Rogerieux F, Boczkowski J, Lacroix G. Biodistribution and Clearance of Instilled Carbon Nanotubes in Rat Lung. Part. *Fibre Toxicol.* 2008; 5:20–32. [PubMed: 19068117]
5. Donaldson K, Murphy FA, Duffin R, Poland CA. Asbestos, Carbon Nanotubes and the Pleural Mesothelium: a Review of the Hypothesis Regarding the Role of Long Fibre Retention in the Parietal Pleura, Inflammation and Mesothelioma. Part. *Fibre Toxicol.* 2010; 7:5–21. [PubMed: 20307263]
6. Chou CC, Hsiao HY, Hong QS, Chen CH, Peng YW, Chen HW, Yang PC. Single-Walled Carbon Nanotubes can Induce Pulmonary Injury in Mouse Model. *Nano Lett.* 2008; 8:437–445. [PubMed: 18225938]
7. Lam CW, James JT, McCluskey R, Hunter RL. Pulmonary Toxicity of Single-Wall Carbon Nanotubes in Mice 7 and 90 Days After Intratracheal Instillation. *Toxicol. Sci.* 2004; 77:126–134. [PubMed: 14514958]

8. Muller J, Huaux F, Moreau N, Mission P, Heilier JF, Delos M. Respiratory Toxicity of Multi-Wall Carbon Nanotubes. *Toxicol. Appl. Pharmacol.* 2005; 207:221–231.
9. Murphy FA, Poland CA, Duffin R, Donaldson K. Length-Dependent Pleural Inflammation and Parietal Pleural Responses After Deposition of Carbon Nanotubes in the Pulmonary Airspaces of Mice. *Nanotoxicol.* 2012 doi: 10.3109/17435390.2012.713527.
10. Mercer RR, Hubbs AF, Scabilloni JF, Wang L, Battelli LA, Schwegler-Berry D, Castranova V, Porter DW. Distribution and Persistence of Pleural Penetrations by Multi-Walled Carbon Nanotubes. Part. *Fibre Toxicol.* 2010; 7:28–38. [PubMed: 20920331]
11. Yang H, Testa JR, Carbone M. Mesothelioma Epidemiology, Carcinogenesis, and Pathogenesis. *Curr. Treat. Options Oncol.* 2008; 9:147–157. [PubMed: 18709470]
12. Puhakka A, Ollikainen T, Soini Y, Kahlos K, Saily M, Koistinen P. Modulation of DNA Single-Strand Breaks by Intracellular Glutathione in Human Lung Cells Exposed to Asbestos Fibers. *Mutat. Res.* 2002; 514:7–17. [PubMed: 11815240]
13. Pacurari M, Yin XJ, Zhao J, Ding M, Leonard SS, Schwegler-Berry D, Ducatman BS, Sbarra D, Hoover MD, Castranova V, et al. Raw Single-Wall Carbon Nanotubes Induce Oxidative Stress and Activate MAPKs, AP-1, NF- κ B, and AKT in Normal and Malignant Human Mesothelial Cells. *Environ. Health Perspect.* 2008; 116:1211–1217. [PubMed: 18795165]
14. Kaiser JP, Wick P, Manser P, Spohn P, Bruinink A. Single Walled Carbon Nanotubes (SWCNT) Affect Cell Physiology and Cell Architecture. *J. Mater. Sci. Mater. Med.* 2008; 19:1523–1527. [PubMed: 17990080]
15. Tabet L, Bussy C, Amara N, Setyan A, Grodet A, Rossi MJ, Pairon JC, Boczkowski J, Lanone S. Adverse Effects of Industrial Multiwalled Carbon Nanotubes on Human Pulmonary Cells. *J. Toxicol. Environ. Health A.* 2009; 72:60–73. [PubMed: 19034795]
16. Bozzuto G, Ruggieri R, Molinari A. Molecular Aspects of Tumor Cell Migration and Invasion. *Ann. Ist. Super Sanità.* 2010; 46:66–80. [PubMed: 20348621]
17. Horwitz R, Webb D. Cell Migration. *Curr. Biol.* 2003; 13:R756–R759. [PubMed: 14521851]
18. Friedl P, Wolf K. Tumor-Cell Invasion and Migration: Diversity and Escape Mechanisms. *Nat. Rev. Cancer.* 2003; 3:362–374. [PubMed: 12724734]
19. Mercer RR, Scabilloni J, Wang L, Kisin E, Murray AR, Schwegler-Berry D, Shvedova AA, Castranova V. Alteration of Deposition Pattern and Pulmonary Response as a Result of Improved Dispersion of Aspirated Single Walled Carbon Nanotubes in a Mouse Model. *Am. J. Physiol. Lung Cell Mol. Physiol.* 2008; 294:L87–L97. [PubMed: 18024722]
20. Shvedova AA, Kisin ER, Mercer R, Murray AR, Johnson VJ, Poapovich AI, Tyurina YY, Gorelik O, Arepalli S, Schwegler-Berry D, et al. Unusual Inflammatory and Fibrogenic Pulmonary Responses to Single-Walled Carbon Nanotubes in Mice. *Am. J. Physiol. Lung Cell Mol. Physiol.* 2005; 289:L698–L708. [PubMed: 15951334]
21. Stone KC, Mercer RR, Gehr P, Stockstill B, Crapo JD. Allometric Relationships of Cell Numbers and Size in the Mammalian Lung. *Am. J. Respir. Cell Mol. Biol.* 1992; 6:235–243. [PubMed: 1540387]
22. Takeuchi T, Nakajima M, Morimoto K. A Human Cell System for Detecting Asbestos Cytogenotoxicity *in vitro*. *Mutat. Res.* 1999; 438:63–70. [PubMed: 9858688]
23. Brown JS, Zeman KL, Bennet WD. Ultrafine Particle Deposition and Clearance in the Healthy and Obstructed Lung. *Am. J. Respir. Crit. Care Med.* 2002; 166:1240–1247. [PubMed: 12403694]
24. Shvedova AA, Kisin E, Murray AR, Johnson VJ, Gorelik O, Arepalli S, Hubbs AF, Mercer RR, Keohavong P, Sussman N, et al. Inhalation vs. Aspiration of Single-Walled Carbon Nanotubes in C57BL/6 Mice: Inflammation, Fibrosis, Oxidative Stress, and Mutagenesis. *Am. J. Physiol. Lung Cell Mol. Physiol.* 2008; 295:L552–L565. [PubMed: 18658273]
25. Li X, Peng Y, Qu X. Carbon Nanotubes Selective Destabilization of Duplex and Triplex DNA and Inducing B–A Transition in Solution. *Nucleic Acids Res.* 2006; 34:3670–3676. [PubMed: 16885240]
26. Sargent LM, Hubbs AF, Young SH, Kashon ML, Dinu CZ, Salisbury JL, Benkovic SA, Lowry DT, Murray AR, Kisin ER, et al. Single-Walled Carbon Nanotube-Induced Mitotic Disruption. *Mut. Res.* 2012; 745:28–37. [PubMed: 22178868]

27. Xu J, Futakuchi M, Shimizu H, Alexander DB, Yanagihara K, Fukamachi K, Suzui M, Kanno J, Hirose A, Ogata A, et al. Multi-Walled Carbon Nanotubes Translocate into the Pleural Cavity and Induce Visceral Mesothelial Proliferation in Rats. *Cancer Science*. 2012; 103:2045–2050. [PubMed: 22938569]
28. Heintz NH, Janssen-Heininger YMW, Mossman BT. Asbestos, Lung Cancers, and Mesotheliomas: From Molecular Approaches to Targeting Tumor Survival Pathways. *Am. J. Respir. Cell Mol. Biol.* 2010; 42:133–139. [PubMed: 20068227]
29. Sharma CS, Sarkar S, Periyakaruppan A, Barr J, Wise K, Thomas R, Wilson BL, Ramesh GT. Single-Walled Carbon Nanotubes Induces Oxidative Stress in Rat Lung Epithelial Cells. *J. Nanosci. Nanotechnol.* 2007; 7:2466–2472. [PubMed: 17663266]
30. Cho SY, Klemke RL. Extracellular-Regulated Kinase Activation and CAS/Crk Coupling Regulate Cell Migration and Suppress Apoptosis During Invasion of the Extracellular Matrix. *J. Cell Biol.* 2000; 149:223–236. [PubMed: 10747099]
31. Friedl P, Brucker EB. The Biology of Cell Locomotion with Three-Dimensional Extracellular Matrix. *Cell Mol. Life Sci.* 2000; 57:41–64. [PubMed: 10949580]
32. Wang L, Luanpitpong S, Castranova V, Tse W, Lu Y, Pongrakhananon V, Rojanasakul Y. Carbon Nanotubes Induce Malignant Transformation and Tumorigenesis of Human Lung Epithelial Cells. *Nano Lett.* 2011; 11:2796–2803. [PubMed: 21657258]
33. Lee AG, Charles AV, Norma JM, Agnes BK. Growth Factor Responses and Protooncogene Expression of Murine Mesothelial Cell Lines Derived from Asbestos-Induced Mesotheliomas. *Toxicol. Pathol.* 1997; 25:565–573. [PubMed: 9437800]
34. Tamaoki J, Isono K, Takeyama K, Tagaya E, Nakata J, Nagai A. Ultrafine Carbon Black Particles Stimulate Proliferation of Human Airway Epithelium *via* EGF Receptor5 Mediated Signaling Pathway. *Am. J. Physiol. Lung Cell Mol. Physiol.* 2004; 287:L1127–L1133. [PubMed: 15298855]
35. Lauffenburger DA, Horwitz AF. Cell Migration: a Physically Integrated Molecular Process. *Cell.* 1996; 84:359–369. [PubMed: 8608589]
36. Guo NL, Wan YW, Denvir J, Porter DW, Pacurari M, Wolfarth MG, Castranova V, Qian Y. Multi-Walled Carbon Nanotube-Induced Gene Signatures in the Mouse Lung: Potential Predictive Value for Human Lung Cancer Risk and Prognosis. *J. Toxicol. Environ. Health A.* 2012; 75:1129–1153. [PubMed: 22891886]
37. Park EJ, Roh J, Kim SN, Kang MS, Han YA, Kim Y, Hong JT, Choi K. A Single Intratracheal Instillation of Single-Walled Carbon Nanotubes Induced Early Lung Fibrosis and Subchronic Tissue Damage in Mice. *Arch. Toxicol.* 2011; 85:1121–1131. [PubMed: 21472445]
38. Passlick B, Sienel W, Seen-Hibler R. Overexpression of Matrix Metalloproteinase 2 Predicts Unfavorable Outcome in Early-Stage Non-Small Cell Lung Cancer. *Clin. Cancer Res.* 2000; 6:3944–3948. [PubMed: 11051242]
39. Tan RJ, Fattman CL, Niehouse LM, Tobolewski JM, Hanford LE, Li QL, Monzon FA, Parks WC, Oury TD. Matrix Metalloproteinases Promote Inflammation and Fibrosis in Asbestos-Induced Lung Injury in Mice. *Am. J. Respir. Cell Mol. Biol.* 2006; 35:289–297. [PubMed: 16574944]
40. Stetler-Stevenson WG, Aznavoorian S, Liotta LA. Tumor Cell Interactions with the Extracellular Matrix During Invasion and Metastasis. *Annu. Rev. Cell Biol.* 1993; 9:541–573. [PubMed: 8280471]
41. Nagase H, Woessner JF Jr. Matrix Metalloproteinase. *J. Biol. Chem.* 1999; 274:21491–21494. [PubMed: 10419448]
42. Birkedal-Hansen H, Moore WG, Bodden MK. Matrix Metalloproteinases: a Review. *Crit. Rev. Oral Biol. Med.* 1993; 4:197–250. [PubMed: 8435466]
43. Coussens LM, Werb Z. Matrix Metalloproteinases and the Development of Cancer. *Chem. Biol.* 1996; 3:895–904. [PubMed: 8939708]
44. Wang A, Zhang B, Huang H, Zhang L, Zeng D, Tao Q, Wang J, Pan C. Suppression of Local Invasion of Ameloblastoma by Inhibition of Matrix Metalloproteinase-2 *in vitro*. *BMC Cancer.* 2008; 8:182. [PubMed: 18588710]
45. Shen YG, Xu YJ, Shi ZL, Han HL, Sun DQ, Zhang X. Effects of RNAi-Mediated Matrix Metalloproteinase2 Gene Silencing on the Invasiveness and Adhesion of Esophageal Carcinoma Cells, KYSE150. *Dig. Dis. Sci.* 2012; 57:32–37. [PubMed: 21879284]

46. Masson V, Ballina LR, Munaut C, Wielockx B, Jost M, Maillard C, Blacher S, Bajou K, Itoh T, Itohara S, et al. Contribution of Host MMP-2 and MMP-9 to Promote Tumor Vascularization and Invasion of Malignant Keratinocytes. *FASEB*. 2004; 19:234–236.
47. Tokuraku M, Sato H, Murakami S, Okada Y, Watanabe Y, Seiki M. Activation of the Precursor of Gelatinase A/72 kDa Type IV Collagenase/MMP-2 in Lung Carcinomas Correlates with the Expression of Membrane Type Matrix Metalloproteinase (MT-MMP) and with Lymph Node Metastasis. *Int. J. Cancer*. 1995; 64:355–359. [PubMed: 7591310]
48. Suzuki M, Kobayashi H, Kanayama N, Saga Y, Suzuki M, Lin CY, Dickson RB, Terao T. Inhibition of Tumor Invasion by Genomic Down-Regulation of Matriptase Through Suppression of Activation of Receptor-Bound Pro-Urokinase. *J. Biol. Chem*. 2004; 279:14899–14908. [PubMed: 14747469]
49. Li H, Daculsi R, Bareille R, Bourget C, Amedee J. uPA and MMP-2 were Involved in Self-Assembled Network Formation in a Two Dimensional Co-Culture Model of Bone Marrow Stromal Cells and Endothelial Cells. *JCB*. 2013; 114:650–657. [PubMed: 23059760]
50. Mi Z, Guo H, Wai PY, Gao C, Kuo PC. Integrin-Linked Kinase Regulates Osteopontin-Dependent MMP-2 and uPA Expression to Convey Metastatic Function in Murine Mammary Epithelial Cancer Cells. *Carcinogenesis*. 2006; 27:1134–1145. [PubMed: 16474180]
51. Xie TX, Huang FJ, Aldape KD. Activation of Stat3 in Human Melanoma Promotes Brain Metastasis. *Cancer Res*. 2006; 66:3188–3196. [PubMed: 16540670]
52. Xie TX, Wei D, Liu M, Gao AC, Osman FA, Sawaya R, Huang S. Stat3 Activation Regulates the Expression of Matrix Metalloproteinase-2 and Tumor Invasion and Metastasis. *Oncogene*. 2004; 23:3550–3560. [PubMed: 15116091]
53. Yu CL, Meyer DJ, Campbell GS, Lamer AC, Carter-Su C, Schwartz J, Jove R. Enhanced DNA-Binding Activity of a Stat3-Related Protein in Cells Transformed by the Src Oncoprotein. *Science*. 1995; 269:81–83. [PubMed: 7541555]
54. Jin EJ, Park KS, Bang OS, Kang SS. Akt Signaling Regulates Actin Organization via Modulation of MMP-2 Activity During Chondrogenesis of Chick Wing Limb Bud Mesenchymal Cells. *JCB*. 2007; 102:252–261. [PubMed: 17551962]
55. Park BK, Zeng X, Glazer RI. Akt1 Induces Extracellular Matrix Invasion and Matrix Metalloproteinase-2 Activity in Mouse Mammary Epithelial Cells. *Cancer Res*. 2001; 61:7647–7653. [PubMed: 11606407]
56. Hu J, Chen C, Su Y, Du J, Qian X, Jin Y. Vascular Endothelial Growth Factor Promotes the Expression of Cyclooxygenase 2 and Matrix Metalloproteinases in Lewis Lung Carcinoma Cells. *Exp. Ther. Med*. 2012; 4:1045–1050. [PubMed: 23226772]
57. Murphy G, Gavrilovic J. Proteolysis and Cell Migration: Creating a Path? *Curr. Opin. Cell Biol*. 1999; 11:614–621. [PubMed: 10508651]
58. Kohn EC, Liotta LA. Molecular Insights into Cancer Invasion: Strategies for Prevention and Intervention. *Cancer Res*. 1995; 55:1856–1862. [PubMed: 7728753]
59. Grigioni WF, D'Errico A, Fortunato C. Prognosis of Gastric Carcinoma Revealed by Interactions Between Tumor Cells and Basement Membrane. *Mol. Pathol*. 1994; 7:220–225.
60. Sáinz-Jaspeado M, Lagares-Tena L, Lasheras J. Caveolin-1 Modulates the Ability of Ewing's Sarcoma to Metastasize. *Cancer Res*. 2010; 8:1489–1500.
61. Tanaka S, Choe N, Iwagaki A, Hemenway DR, Kagan E. Asbestos Exposure Induces MCP-1 Secretion by Pleural Mesothelial Cells. *Exp. Lung Res*. 2000; 26:241–255. [PubMed: 10923243]
62. Shvedova AA, Fabisiak JP, Kisin ER, Murray AR, Roberts JR, Tyurina YY, Antonini JM, Feng WH, Kommineni C, Reynolds J, et al. Sequential Exposure to Carbon Nanotubes and Bacteria Enhances Pulmonary Inflammation and Infectivity. *Am. J. Respir. Cell Mol. Biol*. 2008; 38:579–590. [PubMed: 18096873]
63. Ahmed S, Pakozdi A, Koch AE. Regulation of Interleukin-1 β -Induced Chemokine Production and Matrix Metalloproteinase-2 Activation by Epigallocatechin-3-Gallate in Rheumatoid Arthritis Synovial Fibroblasts. *Arthritis Rheum*. 2006; 54:2393–2401. [PubMed: 16869002]
64. Pan J, Chang Q, Wang X, Son Y, Zhang Z, Chen G, Luo J, Bi Y, Chen F, Shi X. Reactive Oxygen Species-Activated Akt/ASK1/p38 Signaling Pathway in Nickel Compound-Induced Apoptosis in BEAS 2B Cells. *Chem. Res. Toxicol*. 2010; 23:568–577. [PubMed: 20112989]

65. Habibzadegah-Tari P, Byer KG, Khan SR. Reactive Oxygen Species Mediated Calcium Oxalate Crystal-Induced Expression of MCP-1 in HK-2 Cells. *Urol. Res.* 2006; 34:26–36. [PubMed: 16397773]
66. Wang L, Castranova V, Mishra A, Chen B, Mercer RR, Schwegler-Berry D, Rojanasakul Y. Dispersion of Single-Walled Carbon Nanotubes by a Natural Lung Surfactant for Pulmonary *in vitro* and *in vivo* Toxicity Studies. Part. *Fibre Toxicol.* 2010; 7:31–41. [PubMed: 20958985]
67. Wang L, Stueckle TA, Mishra A, Derk R, Meighan T, Castranova V, Rojanasakul Y. Neoplastic Transformation Effect of Single-Walled and Multi-Walled Carbon Nanotubes *vs.* Asbestos on Human Lung Small Airway Epithelial Cells. *Nanotoxicol.* 2013 doi: 10.3109/17435390.2013.801089.
68. Mishra A, Rojanasakul Y, Chen BT, Castranova V, Mercer RR, Wang L. Assessment of Pulmonary Fibrogenic Potential of Multiwalled Carbon Nanotubes in Human Lung Cells. *J. Nanomater.* 2012 doi: 10.1155/2012/930931.
69. Porter DW, Hubbs AF, Mercer RR, Wu N, Wolfarth MG, Sriram K, Leonard S, Battelli L, Schwegler-Berry D, Friend S, et al. Mouse Pulmonary Dose- and Time Course-Responses Induced by Exposure to Multi-Walled Carbon Nanotubes. *Toxicol.* 2010; 269:136–147.
70. Kesanakurti D, Chetty C, Dinh DH, Gujrati M, Rao JS. Role of MMP-2 in the Regulation of IL-6/ Stat3 Survival Signaling *via* Interaction with $\alpha 5\beta 1$ Integrin in Glioma. *Oncogene.* 2013; 32:3275340.
71. Stueckle TA, Lu Y, Davis ME, Wang L, Jiang BH, Holaskova I, Schafer R, Barnett JB, Rojanasakul Y. Chronic Occupational Exposure to Arsenic Induces Carcinogenic Gene Signaling Networks and Neoplastic Transformation in Human Lung Epithelial Cells. *Toxicol. Appl. Pharmacol.* 2012; 261:204–216. [PubMed: 22521957]

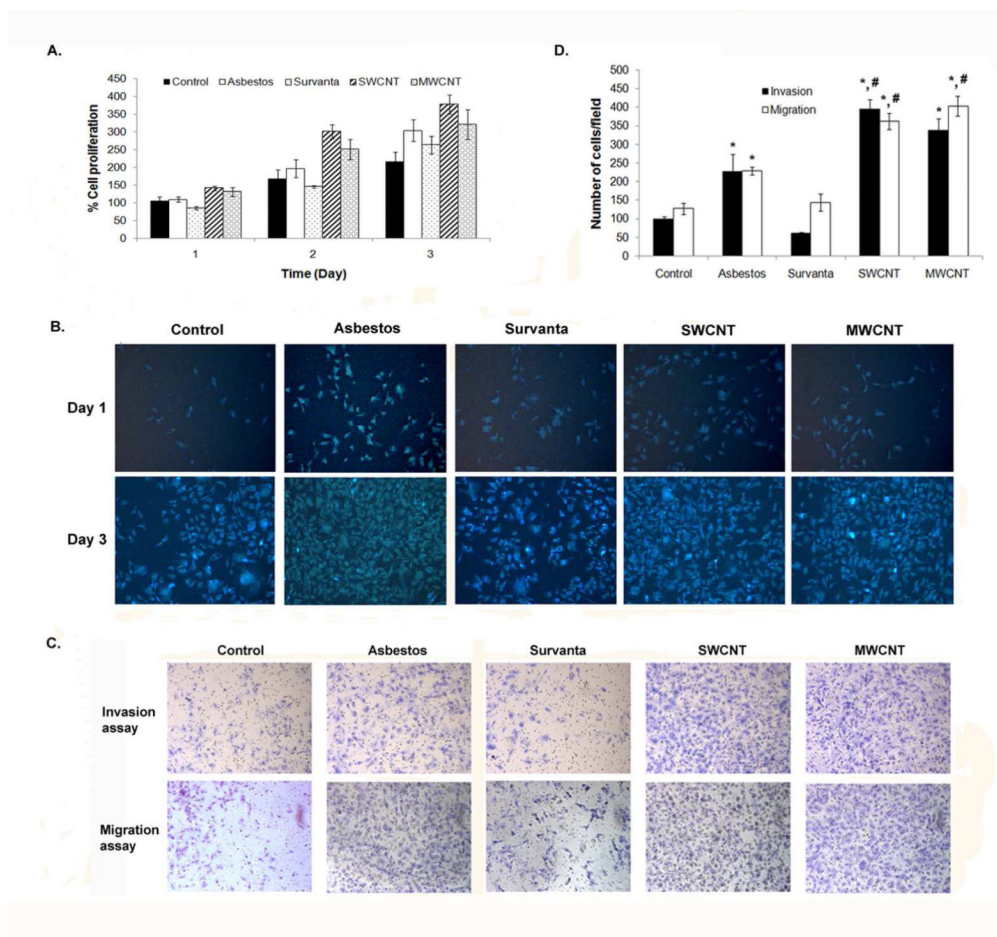


Figure 1.

Chronic exposure to SWCNT, MWCNT and asbestos induces cell proliferation and aggressive behavior of mesothelial MeT5A cells. (A) Passage control (Control), vehicle control (Survanta) and chronic SWCNT, MWCNT or asbestos-exposed cells were seeded in 96 well plate and cell proliferation assay was performed using Cyquant® cell proliferation kit for 3 continuous days. (B) Hoechst 33342 vital stain of passage control, vehicle control and chronic SWCNT, MWCNT or asbestos-exposed cells at 1 and 3 days after seeding. (C) Cell invasion and migration of passage control, vehicle control and chronic SWCNT, MWCNT or asbestos-exposed cells were determined using Transwell® with 8 μ m pore size polycarbonate filter and BD Matrigel® invasion chamber. Cells that invaded or migrated to the lower side of the membrane were stained. (D) The invading and migrating cell numbers were then quantified by counting and depicted as bar charts. * = significant difference from control with $P < 0.05$, # = significant difference from asbestos-exposed cells with $P < 0.05$

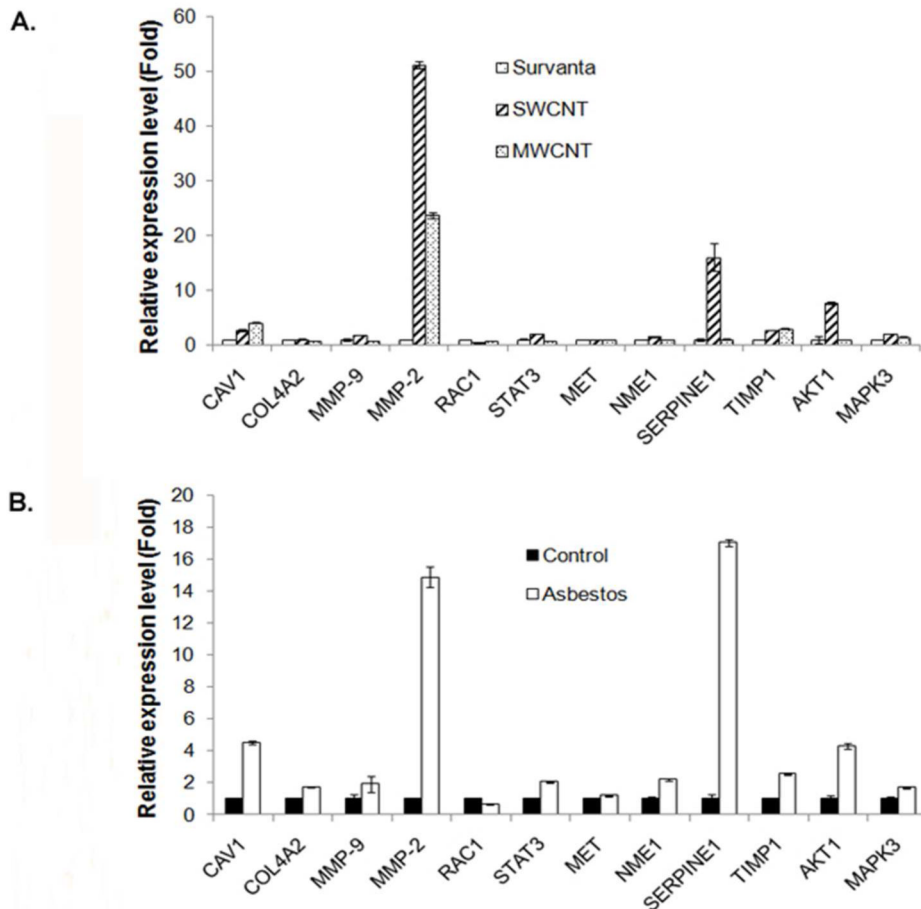


Figure 2.

Elevation of cell invasion and migration regulatory genes in chronic CNT-exposed and asbestos-exposed MeT5A cells. Total RNA was isolated from passage control, vehicle control and chronic SWCNT, MWCNT or asbestos-exposed cells before reverse transcribed into cDNA. The expression of 12 selected genes reported to be involved in cell invasion and migration process including CAV1, COL4A2, MMP-9, MMP-2, RAC1, STAT3, MET, NME1, SERPINE1, TIMP1, AKT1 and *MAPK3* was analyzed by RT-qPCR. The relative expression of each gene to housekeeping gene *18S* in (A) chronic CNT-exposed cells and (B) chronic asbestos-exposed cells compared to vehicle control and passage control cells, respectively, were shown.

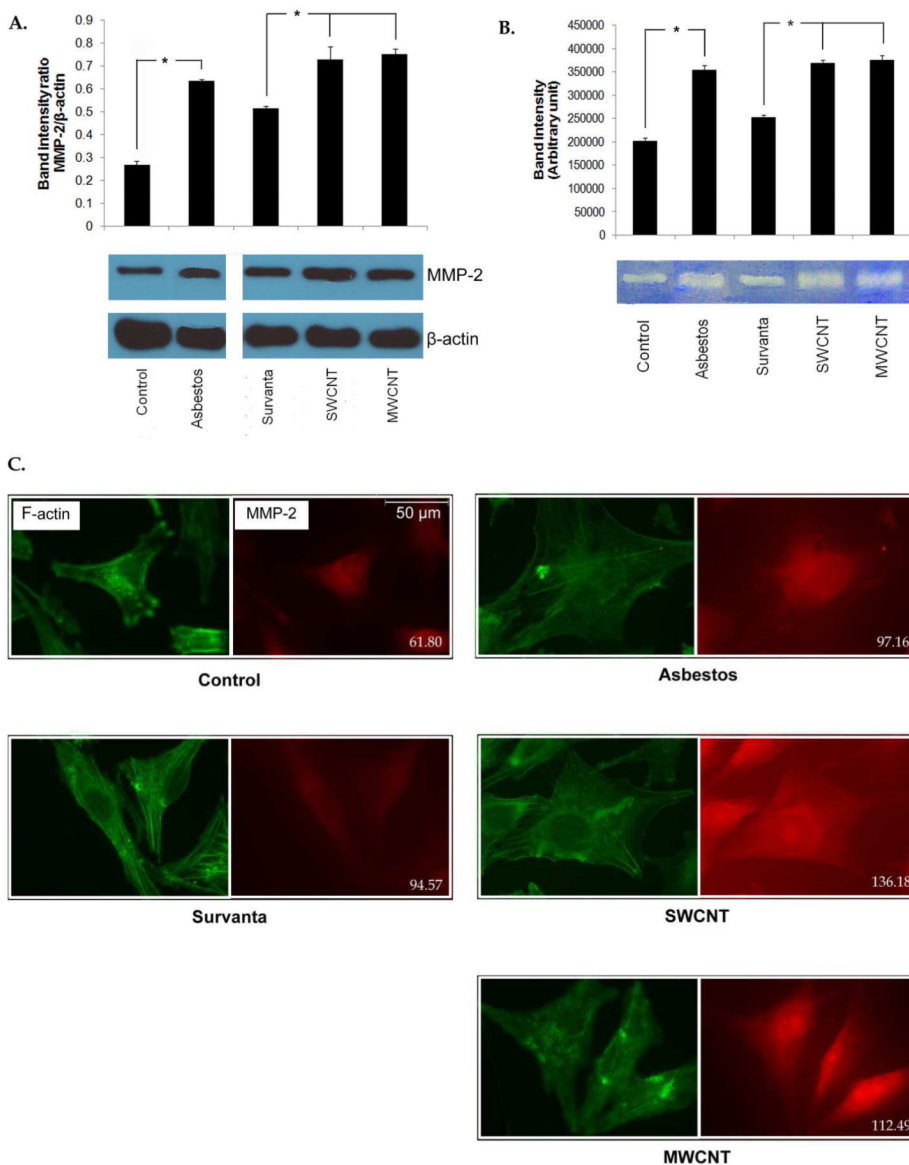


Figure 3. Increased MMP-2 expression and activity in chronic CNT-exposed and asbestos-exposed MeT5A cells. (A) MMP-2 expression in passage control, vehicle control and chronic SWCNT, MWCNT or asbestos-exposed cells was determined by Western blotting. Lysates of each sample were resolved under denaturing conditions by 10% SDS-PAGE and transferred onto PVDF membrane. The membrane was then probed with MMP-2 antibody and detected by enhanced chemiluminescence detection system. * = significant difference with $P < 0.05$ (B) MMP-2 gelatinolytic activity of passage control, vehicle control and chronic SWCNT, MWCNT or asbestos-exposed cells was shown by gelatin zymography. Cell supernatants were collected, resolved by electrophoresis in SDS-polyacrylamide gels containing 0.1% gelatin and stained with 0.5% Coomassie brilliant blue. Densitometry was used to compare enzymatic activity. * = significant difference with $P < 0.05$ (C) Cellular MMP-2 expression was visualized by immunofluorescence staining. Cells were cultured on glass cover slips, fixed in 4% paraformaldehyde and stained for F-actin (green) and MMP-2

(red). MMP-2 expression level represented by red fluorescence intensity per square inches of each sample was indicated at lower right corner of each capture.

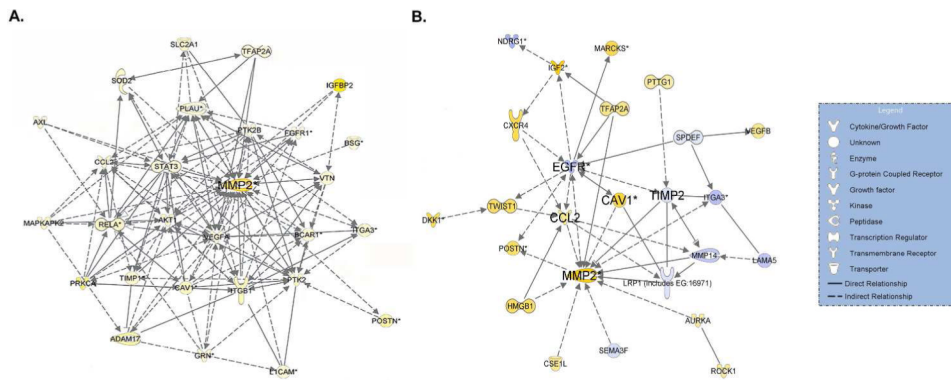


Figure 4. Invasion gene signaling networks (GSNs) of (A) chronic CNT-exposed and (B) chronic asbestos-exposed MeT5A cells. Whole genome expression for each treatment was determined using high-throughput mRNA microarray analysis. Differentially expressed genes (DEGs) were analyzed using Ingenuity Pathway Analysis (IPA) to create pro-invasion GSN. Yellow and blue represent up- and down-regulation, respectively, compared to passage control or vehicle control cells. Color intensity signifies fold change.

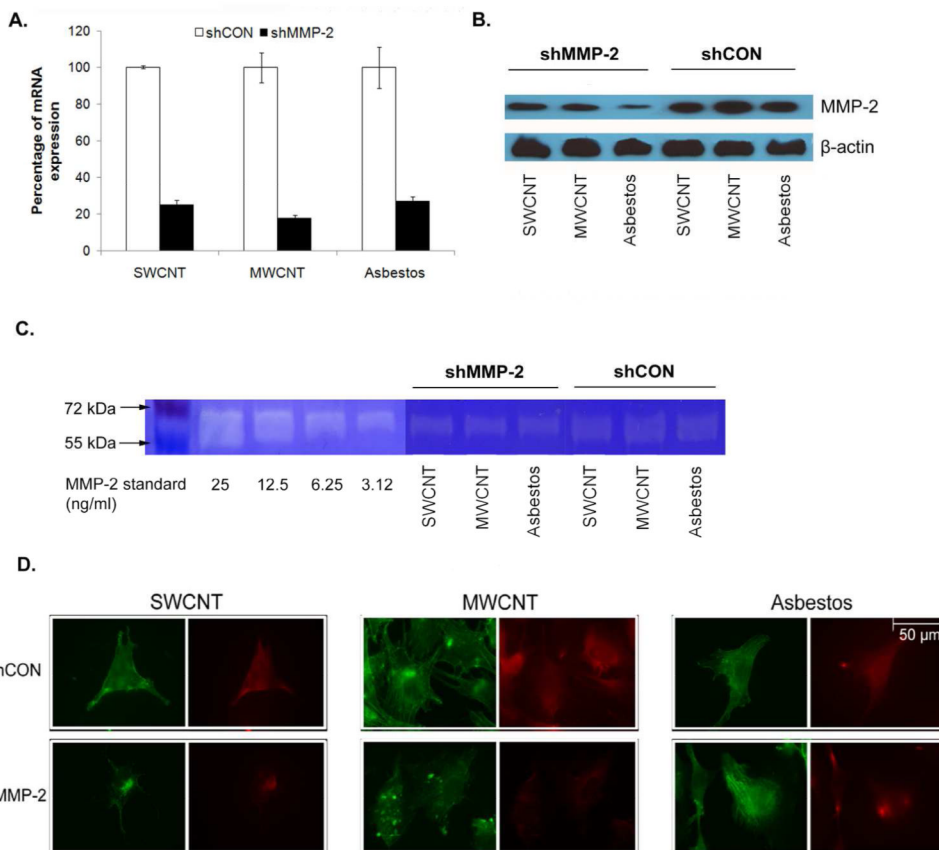


Figure 5. MMP-2 knockdown by shRNA transfection decreases MMP-2 expression and activity in chronic CNT-exposed and asbestos-exposed MeT5A cells. Cells were transfected with pre-designed MMP-2 shRNA (shMMP-2) or scrambled vector (shCON). Stable MMP-2 knockdown clones were generated by puromycin selection. The knockdown efficiency was determined as MMP-2 gene and protein expression of shMMP-2 transfected cells compared to shCON transfected cells by (A) qPCR and (B) Western blot analysis. (C) Gelatinase activity of shMMP-2 transfected and shCON transfected cells demonstrated by gelatin zymography. (D) Immunofluorescence studies further showed the reduction of MMP-2 immunofluorescence intensity in the three shMMP-2-transfected cells compared to shCON transfected cells. F-actin and MMP-2 were stained green and red, respectively.

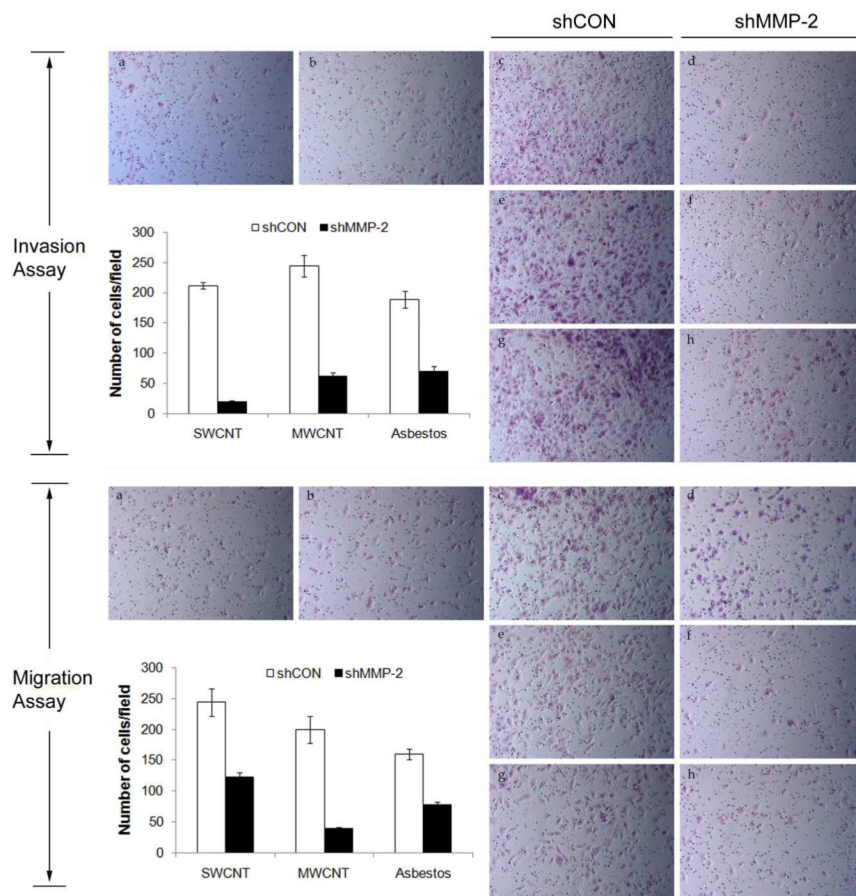


Figure 6. Effects of MMP-2 knockdown on the invasive and migratory activities of chronic CNT-exposed and asbestos-exposed MeT5A cells. Cell invasion and migration of shMMP-2 transfected and shCON transfected cells were determined using Transwell® cell invasion and migration assays. Cells that invaded or migrated to the lower side of the membrane were stained and counted. The number of invading and migrating cells per field was quantified and shown in the bar charts. a = Passage control, b = Vehicle control (Survanta), c and d = SWCNT-exposed cells, e and f = MWCNT-exposed cells, g and h = asbestos-exposed cells